ICES Journal of Marine Science

ICES Journal of Marine Science (2020), 77(1), 408–418. doi:10.1093/icesjms/fsz176

Original Article

Spatial heterogeneity of seasonal phytoplankton blooms in a marginal sea: physical drivers and biological responses

Hongjun Song [1,2,3]*, Rubao Ji[3], Ming Xin[1,2], Ping Liu[1], Zhaohui Zhang[1], and Zongling Wang[1,2]

[1]*Key Lab of Science and Engineering for Marine Ecological Environment, First Institute of Oceanography, MNR, 6 Xianxialing Road, Qingdao 266061, China*
[2]*Laboratory for Marine Ecology and Environmental Science, Qingdao National Laboratory for Marine Science and Technology, 1 Wenhai Road, Qingdao 266237, China*
[3]*Department of Biology, Woods Hole Oceanographic Institution, 266 Woods Hole Road, Woods Hole, MA 02543, USA*

**Corresponding author: tel: + 86 532 6671 7029; e-mail: songhongjun@fio.org.cn.*

Song, H., Ji, R., Xin, M., Liu, P., Zhang, Z., and Wang, Z. Spatial heterogeneity of seasonal phytoplankton blooms in a marginal sea: physical drivers and biological responses. – ICES Journal of Marine Science, 77: 408–418.

Received 13 February 2019; revised 24 August 2019; accepted 1 September 2019; advance access publication 23 September 2019.

Satellite and *in situ* observations are used in this study to examine spatial heterogeneity in the timing and magnitude of phytoplankton blooms in relation to local and remote physical processes in the Yellow Sea (YS), a marginal sea in the northwestern Pacific Ocean. Satellite ocean colour data reveal that annual chlorophyll maximums vary significantly in both timing and magnitude over different subregions of the YS. Strong summer blooms were found off estuary regions, and widespread spring blooms were found in the central trough. Localized autumn and winter peaks were found in small patches around Jeju Island and in nearshore regions. A statistical analysis of *in situ* measurements of the western YS suggests that variability in hydrographic properties could explain most of the spatial heterogeneity observed in both bloom timing and magnitude. The spatial heterogeneity of hydrographic properties, such as stratification and nutrient availability, are controlled by a suite of physical forcings, including the extent of the YS Cold Water Mass, river discharge, warm slope water intrusion, and seasonal warming/cooling. Our results imply that the spatial heterogeneity of marginal seas must be carefully considered when assessing phytoplankton responses in the context of climate change, because of the complexity of underlying mechanisms.

Keywords: physical processes, phytoplankton blooms, spatial heterogeneity, Yellow Sea

Introduction

The spatio-temporal variability of phytoplankton blooms has been studied in many open ocean systems, especially in temperate and subpolar oceans where spring and autumn blooms are most prominent (e.g. Sverdrup, 1953; Legendre, 1990; Siegel *et al.*, 2002; Findlay *et al.*, 2006). It has been widely observed that the timing and magnitude of phytoplankton blooms can vary remarkably across locations and years, largely because of the interactions of multiple physical, chemical, and biological processes (Pingree *et al.*, 1976; Cebrián and Valiela, 1999). In contrast to open oceans, the seascapes of marginal seas are often more complex as a result of biological–physical interactions over finer spatio-temporal scales, forming "mosaic-like" distribution patterns of many biological quantities and processes involving phytoplankton and their blooms.

The underlying mechanisms of seasonal phytoplankton blooms in the open ocean have been explained by many hypotheses (e.g. Sverdrup, 1953; Huisman *et al.*, 1999; Findlay *et al.*, 2006; Behrenfeld, 2010; Chiswell, 2011), where local mixing/stratification processes are considered the key drivers affecting bottom-up and/or top-down control of bloom dynamics. The inflow of remote water masses could play an important role by influencing local water properties and thus influencing phytoplankton bloom dynamics. For example, our earlier studies (Ji *et al.*, 2007; Song *et al.*, 2010) demonstrated that spatial gradients in the timing of both spring and autumn blooms could be

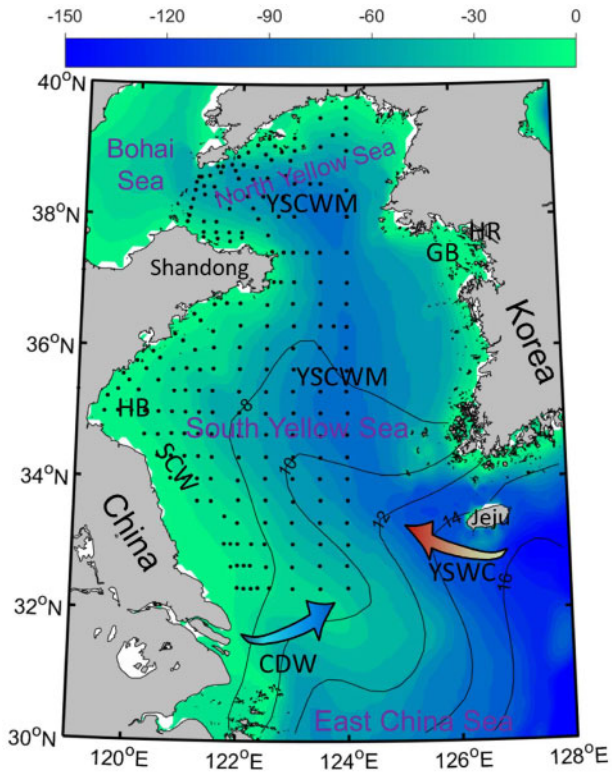

Figure 1. Location and typical water masses of the Yellow Sea (YS). Filled contours with colour bars indicate the bathymetry in metres; black dots denote the observation stations of seasonal cruises for 2006–2007; line contours indicate the surface temperature in February in degrees centigrade; arrows indicate the extension direction of Changjiang Diluted Water (CDW) in the summer and the flow direction of the YS Warm Current (YSWC) in the winter; the YS Cold Water Mass (YSCWM) and Subei Coastal Water (SCW) are also marked; HB, GB, and HR represent the locations of Haizhou Bay, Gyeonggi Bay, and the Han River Estuary, respectively.

influenced by the inflow of upstream water in the Nova Scotian Shelf–Gulf of Maine region. In marginal seas, additional factors such as river run-off coupled with bathymetry gradients can generate habitat heterogeneity by haline-stratification intensity, turbidity, and nutrient conditions and can consequently generate high levels of bloom variability (Rabalais *et al.*, 1996; Zhou *et al.*, 2008).

The Yellow Sea (YS), located between Mainland China and the Korean Peninsula, is a semiclosed marginal sea in the northwestern Pacific (Figure 1). The main water masses and currents in the YS include the YS Cold Water Mass (YSCWM), the YS Warm Current (YSWC), and Changjiang Diluted Water (CDW; e.g. Ho *et al.*, 1959; Lie, 1984; Su and Yuan, 2005). These water masses have unique temperature, salinity, and nutrient characteristics (Wang *et al.*, 2003; Wei *et al.*, 2010), and the seasonal evolution of these water masses can have a strong influence on seasonal phytoplankton blooms (Song *et al.*, 2011; Liu *et al.*, 2015b). For instance, spring phytoplankton blooms in the central YS are likely controlled by the evolution of the YSCWM. Blooms can be initiated as stratification develops and the YSCWM starts to form during spring, followed by strong winter mixing that brings deep, nutrient-rich water to the surface. The blooms then collapse as nutrients at the surface are depleted in a stabilized water column when the YSCWM is fully developed (Hyun and Kim, 2003; Liu *et al.*, 2015b; Wei *et al.*, 2016). It is expected that areas surrounding the central YS present their own bloom dynamics of timing and magnitude owing to additional physical forcings (e.g. CDW and the YSWC). This expectation is supported by some limited (and often indirect) evidence, including that presented by Yamaguchi *et al.* (2012), who reported an areal difference in the seasonal variation in phytoplankton biomass for the YS. However, to the best of our knowledge, very few studies have assessed system-wide variability in bloom dynamics in the YS with a focus on both bloom timing and magnitude. Moreover, there has been almost no quantitative analysis on the mechanisms of bloom variability in this region, especially using *in situ* observations to examine the impact of various environmental conditions.

The main objective of this study is to assess the variability of phytoplankton bloom dynamics in the YS, and identify key biological–physical drivers associated with the spatial heterogeneity of blooms in both timing and magnitude. We first examine the spatial patterns of seasonal phytoplankton blooms from satellite ocean colour data throughout the YS, with respect to both peak timing and magnitude. Then, hierarchical clustering and generalized additive models (GAMs) are used to analyse the field observation data to discern the major environmental factors responsible for the spatial heterogeneity of blooms and to further infer the underlying mechanisms of various physical processes that drive bloom dynamics. From these results, we evaluate the impact of climate-related drivers on bloom variability in the marginal sea, which can thus provide important implications for assessing phytoplankton responses in the context of climate change.

Material and methods

Satellite data

Satellite data analyses were performed to derive the spatial pattern and annual cycle of both chlorophyll *a* (representing phytoplankton biomass) and sea surface temperature (SST). In addition to the NASA standard algorithm (OC4v4-based) chlorophyll product, the remote sensing reflectance (R_{rs}) data were also used as an additional parameter to refine the estimation of chlorophyll concentrations in parts of the YS with high turbidity. The ocean colour data were obtained from NASA Sea-viewing Wide Field-of-view Sensor (SeaWiFS) Level-3 mapped data at a 9-km resolution (http://oceancolor.gsfc.nasa.gov/). Remotely sensed SST data were downloaded from the National Oceanic and Atmospheric Administration's (NOAA's) 1/4° daily optimum interpolation sea surface temperature (OISST) products (https://www.ncdc.noaa.gov/oisst).

Chlorophyll retrieval algorithm

For satellite-retrieved surface chlorophyll, it is known that for coastal waters with high concentrations of suspended particles and coloured dissolved organic matter, NASA's standard product is not directly applicable. As recommended in previous works of the YS (Siswanto *et al.*, 2011; Yamaguchi *et al.*, 2013), a Tassan-like (1994) algorithm and the NASA standard algorithm (OC4v4) were used to obtain chlorophyll concentrations for data with high (>2.5 mW cm^{-2} μm^{-1} sr^{-1}) and low (<1.5 mW cm^{-2} μm^{-1} sr^{-1}) ranges of normalized water-leaving radiance at 555 nm (nLw_{555}), respectively. For data with mid-range nLw_{555} levels (1.5∼2.5 mW

$cm^{-2}\,\mu m^{-1}\,sr^{-1}$), the weighted mean value of chlorophyll determined from the two algorithms was used to keep the data in smooth transition where the weights were subject to a magnitude of nLw_{555}. The Tassan-like algorithm was applied as follows:

$$\log_{10}(\mathrm{Chl}) = -0.166 - 2.158\log_{10}(R) + 9.345\log_{10}{}^{2}(R), \quad (1)$$

$$R = (R_{rs443}/R_{rs555})(R_{rs412}/R_{rs490})^{-0.463}, \quad (2)$$

where R is a function of spectra value and $R_{rs}(\lambda)$ is the remote sensing reflectance value at a given wavelength. The abovementioned hybrid algorithm (combining OC4v4-based and Tassan-like algorithms) was validated in Yamaguchi *et al.* (2013). The resulting chlorophyll concentrations for 1998–2010 were used to compute the climatological mean. Peak timing and magnitude values were chosen as key bloom indices. The peak timing (T_{CM}) is defined as the month with the highest chlorophyll concentration, whereas the bloom magnitude (Chl_{PM}) is defined as the monthly mean chlorophyll concentration of T_{CM}. Based on spatial patterns of bloom timing, eight zones were selected to analyse annual patterns in the central regions with different bloom peak months in the YS, and areal mean chlorophyll concentrations were used to determine the annual time-series.

Field data drawn from cruises

Survey data were used to examine the environmental factors that may control blooms. Environmental data for the western side of the YS were obtained from four seasonal cruises from 2006 to 2007. The cruises sailed in July/August 2006, January/February 2007, April 2007 and October/November 2007, respectively. Sampling stations were positioned in the western part of the YS as shown in Figure 1. The dataset includes profiles for temperature, salinity, total suspended solids (TSS), dissolved inorganic nitrogen (DIN), phosphate (PO_4), and silicate (SiO_3). The sampling methods used are described in previous works (e.g. Fu *et al.*, 2009; Xin *et al.*, 2015).

Statistical analysis

Hierarchical cluster analysis and GAMs were used to assess the degree to which the different environmental conditions were associated with bloom dynamics. Bathymetric (depth, Dep), hydrological (sea surface temperature/salinity, SST/SSS), and chemical (DIN, PO_4, SiO_3, and TSS) parameters were considered, and their annual mean values were used to examine spatial variability. Hierarchical clustering, one of the clustering techniques most commonly used in ecological studies (Clarke *et al.*, 2016), was used to organize the stations into a binary tree that grouped distinct subsets based on their similarity in environmental conditions. The clustering results were applied to compare station groups with different blooms. The function clustergram available from the MATLAB bioinformatics toolbox with standardized Euclidian distances and average linkages for the dendrogram was used, and the results are shown as heat map diagrams. Here the average linkages refer to the average distance between each point in one cluster to every point in the other cluster. GAMs developed by Wood (2006) were used to model the functional relationship between Chl_{PM} and surface environmental factors. A tensor product spline (*te*) was used to measure multiplicative effects between SST and SSS interactions, as they are measured in different units (Wood, 2006). The *te*(SST, SSS) term was made similar to that of a temperature–salinity diagram to identify various water masses. The backward stepwise approach was applied to remove insignificant variables, and the generalized cross-validation score was employed to assess the model's performance. The "gam" function available through the R package "mgcv" was used for GAM analysis and plotting.

Results

Spatial variability of blooms from satellite data

General spatial patterns of the peak month and magnitude of seasonal phytoplankton blooms are presented in Figure 2. Annual maximum chlorophyll concentrations mostly occur in April in the YS's central trough, generally overlapping with the area where the YSCWM is observed during warm seasons (Park *et al.*, 2011). The summer chlorophyll maximum (June to August) is mainly distributed across the waters off the Changjiang Estuary and along the west coast of the Korean Peninsula (including Gyeonggi Bay, the estuary of the Han River), suggesting a strong impact of river inputs on bloom timing. The waters that exhibit autumn chlorophyll maximums (September to November) cover a relatively small area, located mainly around Jeju Island and in some patches of coastal waters. In addition, some subregions with winter chlorophyll maximums (December to February) mainly appear in the nearshore areas of the YS. The results demonstrated the unique spatial pattern of the timing of phytoplankton blooms in the YS: the peak timing of chlorophyll is not synchronized across the YS; rather, it can occur during any of the four seasons depending on the location within the YS. In addition to the strong spatial heterogeneity of peak bloom timing observed, the mean chlorophyll concentration in the peak month increases from the open sea to coastal waters, and reaches a maximum off the Changjiang Estuary (Figure 2b). The Chl_{PM} magnitudes of spring blooms in the central YS largely vary within a range of 1.0∼4.0 mg m^{-3} (averaging ∼2.5 mg m^{-3}), and summer blooms vary within magnitudes of 1.0∼10.0 mg m^{-3} (averaging ∼3.8 mg m^{-3}). Autumn/winter blooms in the nearshore area are much stronger than those in the open sea, e.g. Chl_{PM} concentrations in A1/W1 and A2/W2 Zones are valued at 1.92/2.13 and 0.89/0.73 mg m^{-3}, respectively. The low Chl_{PM} magnitude observed in the southeastern YS is likely a result of relatively low-nutrient levels in this region (Wang *et al.*, 2003; Jang *et al.*, 2013).

The seasonality of chlorophyll for the eight zones specified in Figure 2a is shown in Figure 3. For spring bloom in the central area of the south YS (Zone Sp1), peak timing occurs in early April, and average chlorophyll concentrations from March to April (bloom period) are measured at 1.91 mg m^{-3} (Figure 3a). In the western area of the north YS (Zone Sp2, Figure 3b), a spring bloom occurs earlier (peak timing in late March) and is stronger (∼2.91 mg m^{-3} of mean chlorophyll during March and April) than that observed in Zone Sp1. In waters off the Changjiang Estuary (Zone Su1, Figure 3c), peak chlorophyll levels are observed in July, and the corresponding magnitude is considerably higher (>10 mg m^{-3} on some days). For the summer bloom occurring in Gyeonggi Bay (Zone Su2), the chlorophyll maximum occurs in August (later than that in Zone Su1), and the mean chlorophyll concentration reaches ∼5.24 mg m^{-3} (Figure 3d). For Zone A1 (Figure 3e) south of the Shandong Peninsula, chlorophyll concentrations increase rapidly in September and reach a maximum level in October (monthly

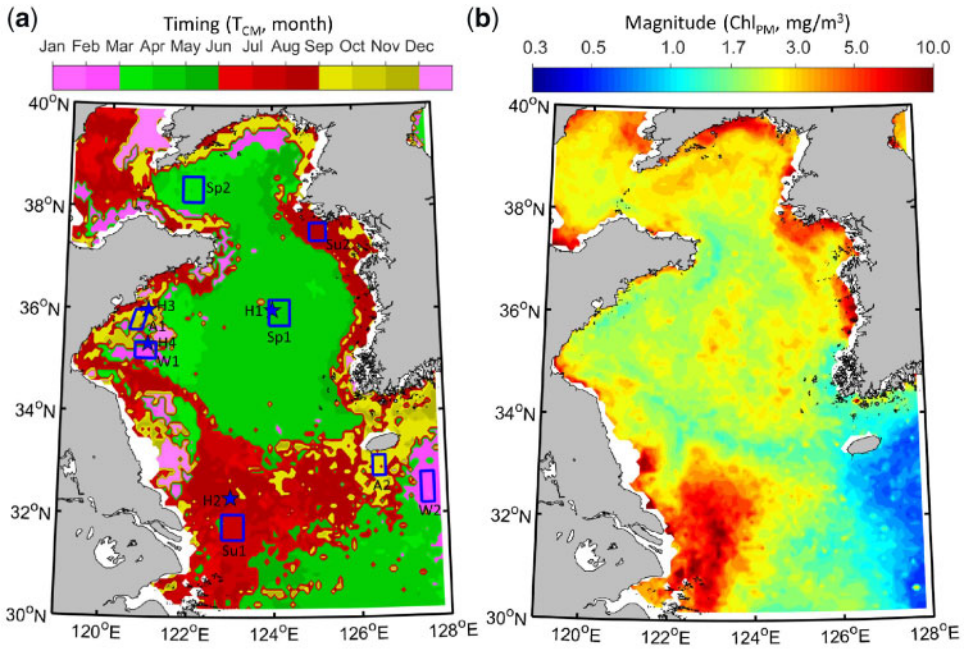

Figure 2. Spatial distribution of bloom timing and magnitude in the Yellow Sea. Climatological chlorophyll data derived from a hybrid algorithm (see the text for details). (a) The month of peak chlorophyll is selected as the bloom timing index; rectangles denote the zones selected for data analysis; Sp1 and Sp2, Su1 and Su2, A1 and A2, and W1 and W2 denote spring, summer, autumn, and winter bloom zones, respectively; pentagrams denote the stations employed for environmental data analysis (H1–H4). (b) The mean chlorophyll concentration in the peak month is selected as the bloom magnitude index.

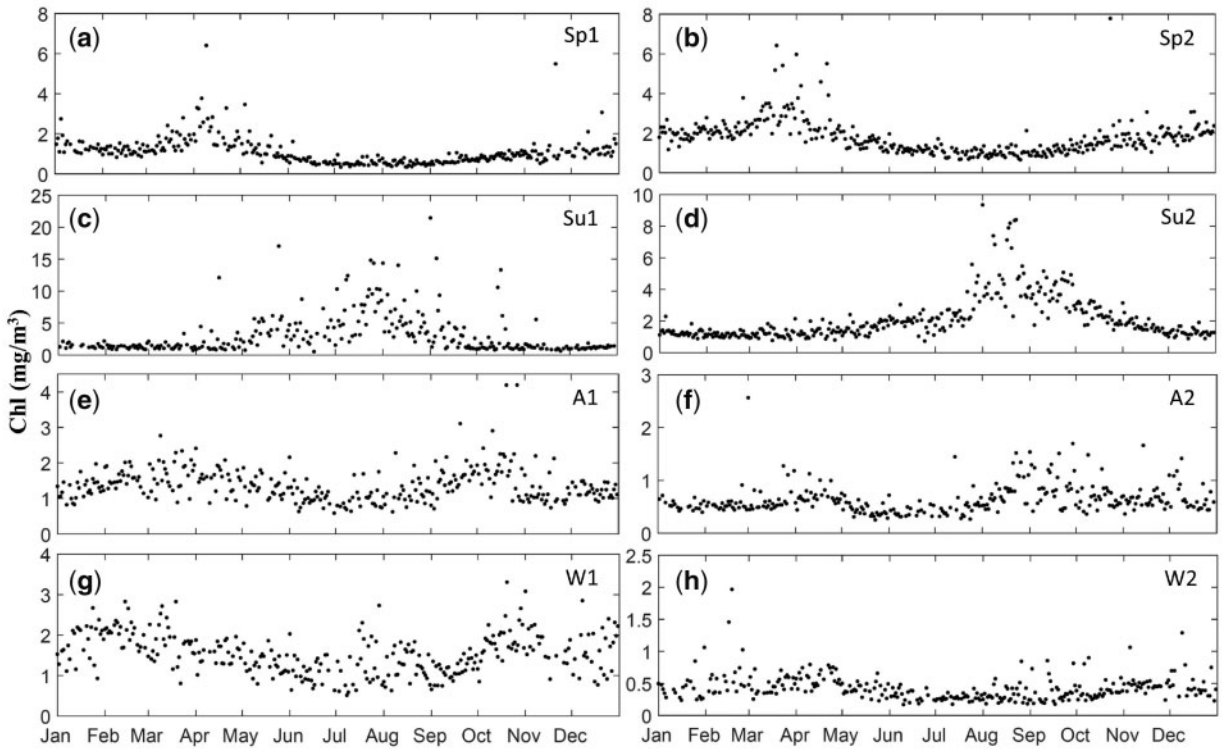

Figure 3. Time-series of daily chlorophyll for the eight zones (a-h) specified in Figure 2a. Each data point denotes the climatological mean of the chlorophyll concentration measured from each zone. Note that the *y*-axes have different ranges.

Table 1. Summary of ship-based survey observations of seasonal phytoplankton blooms and their influencing factors for the YS.

Locations	Phytoplankton	Related physical forcing	References
Central north Yellow Sea	High Chl *a* in spring and autumn	Yellow Sea Cold Water Mass	Gao (2009)
Central south Yellow Sea	Highest Chl *a* in spring	Yellow Sea Cold Water Mass	Fu *et al.* (2010) and Liu *et al.* (2015b)
Off the Changjiang Estuary	Highest Chl *a* in the summer	Changjiang Diluted Water	Fu *et al.* (2009) and Song *et al.* (2014)
Gyeonggi Bay	Blooms in spring and late summer	Fresh-water inflows from the Han River	Choi and Shim (1988) and Yang *et al.* (2008)
Western coast of Jeju	Spring and autumn blooms	Yellow Sea mixed waters	Affan *et al.* (2007) and Kim *et al.* (2009)
Southern coast of Shandong	High Chl *a* in autumn and winter	Lubei Coastal Current	Fu *et al.* (2009) and Wei *et al.* (2016)
Haizhou Bay	Highest abundance in autumn	Subei Coastal Water	Yang *et al.* (2014) and Wei *et al.* (2016)

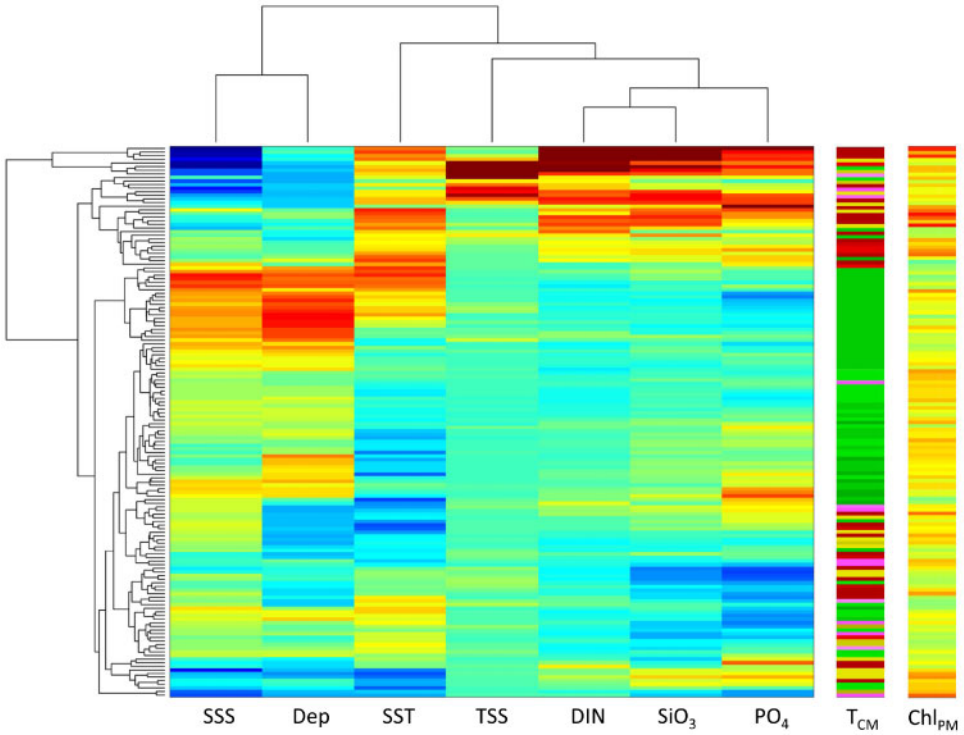

Figure 4. Heat maps showing a cluster tree of various environmental parameters (left) and the corresponding timing and magnitude of blooms (right two). Blue/red colours shown in the cluster tree indicate low/high values of the environmental parameters. Colours shown in the two bar plots on the right are consistent with Figure 2.

mean of 2.13 mg m^{-3}). In the waters surrounding Jeju Island, there is a major autumn bloom and a minor spring bloom (Zone A2, Figure 3f), but the magnitudes of both blooms are relatively weak (peak chlorophyll levels of <2.00 mg m^{-3}). The annual chlorophyll cycle observed in Zone W1 is similar to that found in Zone A1 because of the proximity of their locations with peak timing occurring later on (peak in winter) and with similar magnitude (~2.0 mg m^{-3}, Figure 3g). In Zone W2 outside of the YS, chlorophyll concentrations remain relatively low throughout the whole year (<0.9 mg m^{-3}) with the exception of several enhancements occurring in February (Figure 3h).

Relationship between environmental factors and the spatial heterogeneity of blooms

Previous studies based on *in situ* observations (Table 1, the general location is given in Figure 1) further verify the spatial heterogeneity of blooms in the YS (e.g. spring blooms in the central YS, summer blooms forming off the Changjiang Estuary and in Gyeonggi Bay, spring/autumn blooms surrounding Jeju Island, and autumn/winter blooms along the southern Shandong coast and Haizhou Bay), which are highly consistent with the remotely sensed results shown in Figure 3. Physical processes occurring in the YS (e.g. the YSCWM, CDW, and coastal currents) have been identified as key drivers of these seasonal blooms in the studies listed in Table 1.

In situ environmental data available from seasonal cruises from 2006 to 2007 (station locations shown in Figure 1, mainly in the western YS) were used to examine the impact of environmental factors on bloom dynamics. The cluster analysis shows that SSS and depth are the two key parameters used for environmental grouping followed by SST, TSS, and nutrients (Figure 4). The clusters generated by environmental dissimilarity are compared across subregions with different bloom features. Spring-bloom subregions generally feature high SSS and deep bathymetry (YSCWM region), whereas summer-bloom subregions present

low SSS, shallow bathymetry, high SST, and high nutrients (the CDW region). Subregions with autumn and winter blooms coincide with clusters associated with low salinity and shallow depth conditions, consistent with the nearshore area of the western YS. Moreover, subregions with high peak magnitudes appear to coincide with shallow depths and low salinity clusters representing the coastal regions positioned near estuaries (shown in Figure 2b).

The GAM analysis shows that the environmental parameters employed can explain most of the spatial variability observed in bloom peak magnitude ($\log_{10}$-transformed Chl_{PM}; Table 2). In comparing full models 1 and 2, we find that the one with a tensor product spline of SST and SSS (model 2) slightly improves the model's performance. Strong correlations between explanatory variables (collinearity problems) exist in this case, e.g. between SSS and DIN, DIN and SiO_3, DIN and PO_4, and PO_4 and SiO_3 (correlation coefficients of >0.7 or <-0.7), mainly because of the influence of fresh-water inputs. Thus, the individual effects of available environmental factors are captured by a single explanatory variable in the model, as shown in models 3–10 listed in Table 2. The results show that *te*(SST, SSS) can explain most of the variance in bloom magnitude ($R^2 = 0.475$) among the individual effects, followed by SiO_3, DIN, SSS, SST, Dep, and PO_4. The functional relationships between bloom magnitudes and the main individual environmental parameters are shown in Figure 5. We find a strong positive relationship between bloom magnitude and nutrients, whereas negative effects are found for salinity and depth. SST seems to have a relatively nonmonotonic effect on the bloom magnitude in the YS.

Four stations within representative zones of the seasonal chlorophyll maximum were selected for a comparative study (locations are shown in Figure 2a, and results are shown in Figure 6). The general seasonal cycle of SSTs is similar at all four stations, with higher values in the summer and lower values in spring and winter. The SSS measured at station H2 is relatively low in the summer because of the influence of CDW. Density differences from 30 m to the surface layers also show clear seasonality in stratification, which is weak in the winter, strong in the summer and moderate in spring. In autumn, weak stratification appears at station H3, but the other three stations are well mixed, similar to what is observed in the winter. As they are influenced

Table 2. Statistical results of generalized additive models.

Model	R^2	GCV	*n*
(1) $\log Chl_{PM} \sim s(Dep)+s(SST)+s(SSS)+s(DIN)+s(PO_4)+s(SiO_3)+s(TSS)$	0.639	0.006	154
(2) $\log Chl_{PM} \sim s(Dep)+te(SST, SSS)+s(DIN)+s(PO_4)+s(SiO_3)+s(TSS)$	0.666	0.006	154
(3) $\log Chl_{PM} \sim te(SST, SSS)$	0.475	0.007	191
(4) $\log Chl_{PM} \sim s(SiO_3)$	0.241	0.010	181
(5) $\log Chl_{PM} \sim s(DIN)$	0.212	0.010	195
(6) $\log Chl_{PM} \sim s(SSS)$	0.166	0.010	191
(7) $\log Chl_{PM} \sim s(SST)$	0.144	0.012	192
(8) $\log Chl_{PM} \sim s(Dep)$	0.087	0.012	213
(9) $\log Chl_{PM} \sim s(PO_4)$	0.075	0.012	180
(10) $\log Chl_{PM} \sim s(TSS)$	–	–	172

The full models (1–2) and submodels (3–10) are listed. R^2, the proportion of variance in bloom magnitude explained by the model; GCV, the generalized cross-validation score; *n*, the number of data points available for constructing a specific model; *s*, the thin plate regression spline; *te*, the tensor product spline; –, no significant relationship.

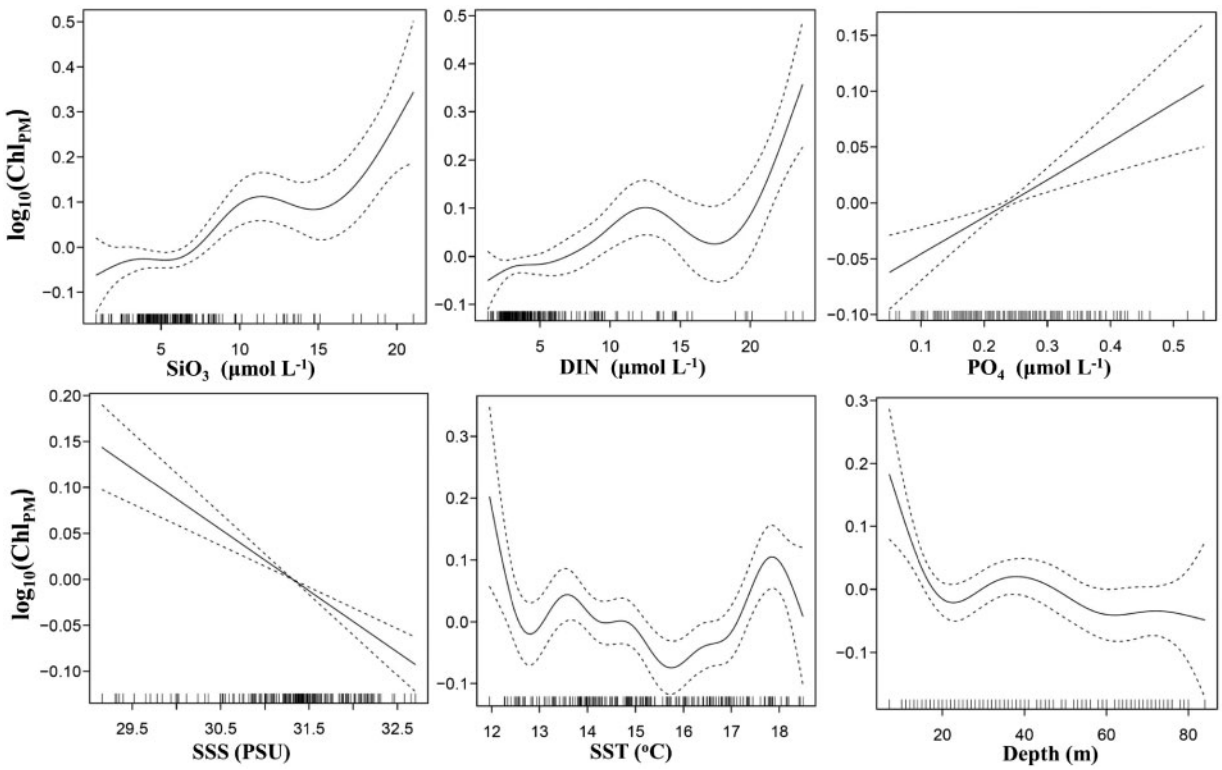

Figure 5. Functional response of bloom magnitude to the main individual environmental factors from models 4–9 in Table 2. Dashed lines indicate 95% confidential intervals.

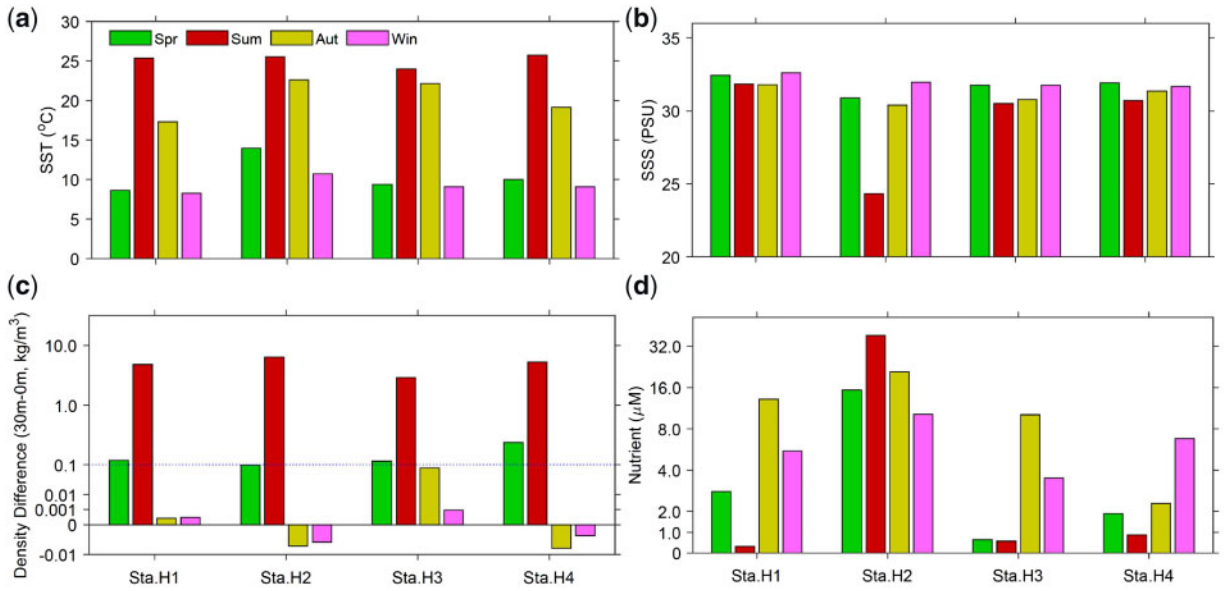

Figure 6. Seasonal comparison of (a) sea surface temperature (SST), (b) sea surface salinity (SSS), (c) density difference (30 m−0 m) and (d) surface nutrients observed in different typical seasonal chlorophyll maximum zones. The observed data were collected from seasonal cruises running from 2006 to 2007. Nutrient data are represented as nitrate concentrations. The locations of stations H1–H4 are specified in Figure 2a. A density difference of 0.1 kg m^{-3} relative to the surface was considered the mixed layer.

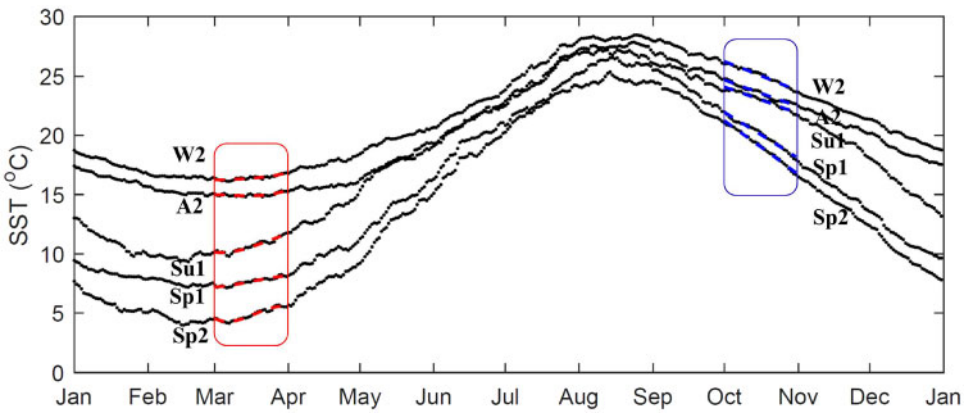

Figure 7. Comparison of seasonal SST variations in the five typical zones specified in Figure 2a.

by various physical forcings, surface nutrients (nitrate concentrations) present different patterns of seasonality at the four stations (Figure 6d): in the central YS (station H1), surface nutrients in the summer are much lower than those observed in the other three seasons because of the stratification-induced inhibition of bottom-to-surface nutrient supplies; fresh-water discharge from Changjiang can keep nutrient levels high throughout the year in waters off the Changjiang Estuary (station H2), with the highest nutrient levels found in the summer because of a high discharge volume; for stations H3 and H4, nutrient concentrations in autumn and winter are higher than those in spring and summer, which is consistent with high chlorophyll levels in autumn and winter (see Zones A1 and W1 in Figure 3e and g), respectively.

Seasonal variations in SST were examined to measure the impact of climate change on bloom heterogeneity. Spring bloom found in Zone Sp2 in the north YS appears earlier and is stronger than that observed in Zone Sp1 in the South YS, possibly because of relatively rapid warming occurring in March in Zone Sp2 (monthly increment: 0.95°C, Figure 7). Slow and late warming inhibits spring bloom as observed in Zones A2 and W2. Weak autumn blooms in Zones Sp1 and Sp2 are also thought to be related to rapid cooling (October decrement: Sp1−4.05°C; Sp2−4.38°C), as indicated by strong mixing in these regions (Figure 6c). However, rapid warming/cooling in spring/autumn may not work in the other bloom zones, such as the summer-bloom zone Su1 and the winter-bloom zone W2.

Discussion

Spatial patterns of the month with the chlorophyll maximum clearly distinguish all four seasonal phytoplankton blooms observed across different subregions of the YS: spring blooms occur in the central trough and cover much of the YS, summer blooms are mainly distributed in waters off the Changjiang Estuary and on the west coast of the Korean Peninsula, and autumn/winter

blooms are mainly positioned around Jeju Island and in some areas of coastal waters. Different biological and physical mechanisms are responsible for bloom seasonality in different regions. The following discussion mainly focuses on how local and remote processes control bloom seasonality.

Blooms controlled by local and remote processes

Spring bloom occurring in the central YS, similar to blooms found in many other temperate-subpolar systems, can be understood as a one-dimensional process driven by the combined effects of nutrient replenishment from winter mixing, increasing temperature and light availability, and the stabilization of the water column (e.g. Sverdrup, 1953; Miller, 2004; Winder and Cloern, 2010). It is evident at station H1 in the central YS (Figure 6) that nutrient concentrations in spring are still high as vertical stratification starts to develop, separating warm surface water and cold deep water masses of the YSCWM. The bloom diminishes in the summer as nutrients are depleted at the surface while nutrient supplies from deeper water are not accessible because of strong thermal stratification.

The bloom positioned off the Changjiang Estuary differs from a typical one-dimensional process. Although the associated phytoplankton source and sink dynamics involve a one-dimensional process, the process leading to vertical stratification and nutrient supplies largely involves horizontal transport. Strong haline stratification and rich nutrients in the summer (as is shown from Sta.H2 in Figure 6) because of significant fresh-water inputs, can sustain the bloom for a long period and form a higher peak in the summer (rather than in spring) in the Changjiang Estuary and in adjacent coastal waters. An *in situ* data analysis shows that nutrient variability is the main factor that controls phytoplankton biomass in waters off the Changjiang Estuary (Song *et al.*, 2014). A similar summer-bloom regime can be found within and close to Gyeonggi Bay, the largest estuary on the west coast of the Korean Peninsula, which receives a large influx of fresh-water from the Han River during the wet summer season (Jahan and Choi, 2014). Our results also suggest that the summer bloom off the Changjiang Estuary is stronger and lasts longer than that occurring in Gyeonggi Bay (Figure 3c and d), likely because of considerable differences in the volume and content of discharged water. In addition, the absence of spring blooms in the estuary region is likely a result of light limitation associated with high sediment concentrations in the water column, resuspended from the bottom because of strong wind- and tide-induced mixing during the winter/spring period (Chen *et al.*, 2006; Yuan *et al.*, 2008).

Similarly, blooms in the YS may also be affected by inflows of the YSWC, which represents a northwestward intrusion of warm and saline water from the open ocean (e.g. Hsueh, 1988; Yuan *et al.*, 2008). The intrusion of the YSWC during cold seasons can inhibit the eastward expansion of CDW (Hyun and Kim, 2003) and thus may be responsible for low-nutrient levels and low bloom magnitudes (Figure 2b) in the southeastern YS (Chen, 2009; Liu *et al.*, 2015a). As a branch of the Kuroshio Current, YSWC is carrying low-nutrient warm surface water (e.g. Ichikawa and Beardsley, 2002; Zhang *et al.*, 2007; Xu *et al.*, 2019). This can also be suggested by indirect evidence from the low chlorophyll concentration year round in Zone W2 (Figure 3h), which shares the same source water as the YSWC. Moreover, the winter bloom in Zone W2, indicated by the relatively sparse data points of elevated chlorophyll concentration during winter in the climatological time-series (Figure 3h), is likely caused by episodic winter-storm-induced mixing and transient supply of nutrients. Overall, the YSWC intrusion is responsible for weak blooms in the southeastern YS.

A bloom can also form when high-biomass water is transported to the area of interest through a three-dimensional process rather than a one-dimensional vertical process (e.g. Lucas *et al.*, 1999). We suggest that this may be the case for autumn bloom forming in waters around Jeju Island (Figure 3f). Autumn blooms are generally considered a result of local effects through the enhancement of vertical mixing-induced nutrient supplies during the summer–winter transition (Findlay *et al.*, 2006). However, this general concept might not be applicable in our case. Rather, the remote supply of biomass generated through the horizontal advection of CDW could play a more important role. In the summer, CDW flows eastward from the Changjiang Estuary and takes 1–2 months to reach the eastern coast of Jeju Island as suggested in previous studies (e.g. Beardsley *et al.*, 1985; Chang and Isobe, 2003). The time-lag is consistent with the difference in bloom formation measured between Zones Su1 and A2 (Figure 3), which is also consistent with the results of an interannual case study by Yamaguchi *et al.* (2012). The area around Jeju Island presents a weak spring bloom, partially resulting from enhanced levels of springtime stratification in the region (Kim *et al.*, 2009).

Links to climate impacts

Seasonal warming and cooling may not only affect physiological phytoplankton processes but may also change stratified conditions in ways that control bloom dynamics (Sarmiento *et al.*, 2004; Winder and Sommer, 2012). Our results have shown that Zone Sp2 in the North YS, which is characterized by relatively rapid surface warming, exhibits an earlier and stronger spring bloom than that found in Zone Sp1 in the South YS. Meanwhile, rapid cooling might be responsible for the weak autumn blooms observed in both zones. Stratification driven by rapid warming can maintain rapid phytoplankton growth because of the light and nutrient advantages of surface waters. A similar explanation can be applied to the impact of slow warming on the weak spring bloom observed in Zone A2. This study reveals a remarkable level of spatial heterogeneity in phytoplankton blooms in this marginal sea, and it cautions against assessing the impact of large-scale climate forcings on bloom dynamics. For different seasonal blooms, bottom-up responses may vary spatially. For example, under future climate scenarios, seasonal warming/cooling rates in spring/autumn could be intensified in the YS. This could promote the development of an earlier spring bloom and further weaken autumn bloom in the central area, and potentially enhance the growth rate and thus the magnitude of the winter bloom in the warmer coastal water. However, in the summer-bloom region, changes in the seasonal warming/cooling rate likely play a less important role than river run-off variability.

The spatial heterogeneity of blooms highlighted in this study has important implications. First, drivers of this heterogeneity vary spatially. Some drivers are climate-specific, such as mixing/stratification and fresh-water discharge, whereas the others are not (e.g. bathymetry, Liu and Wang, 2013). Even climate-related factors can vary in magnitude and may spur different biological responses. However, large-scale climate models often cannot adequately resolve marginal sea systems (Stock *et al.*, 2011; Holt *et al.*, 2017) and require a certain degree of simplification and parameterization. We argue that this requirement will limit the application of such models in projecting future ecosystem changes

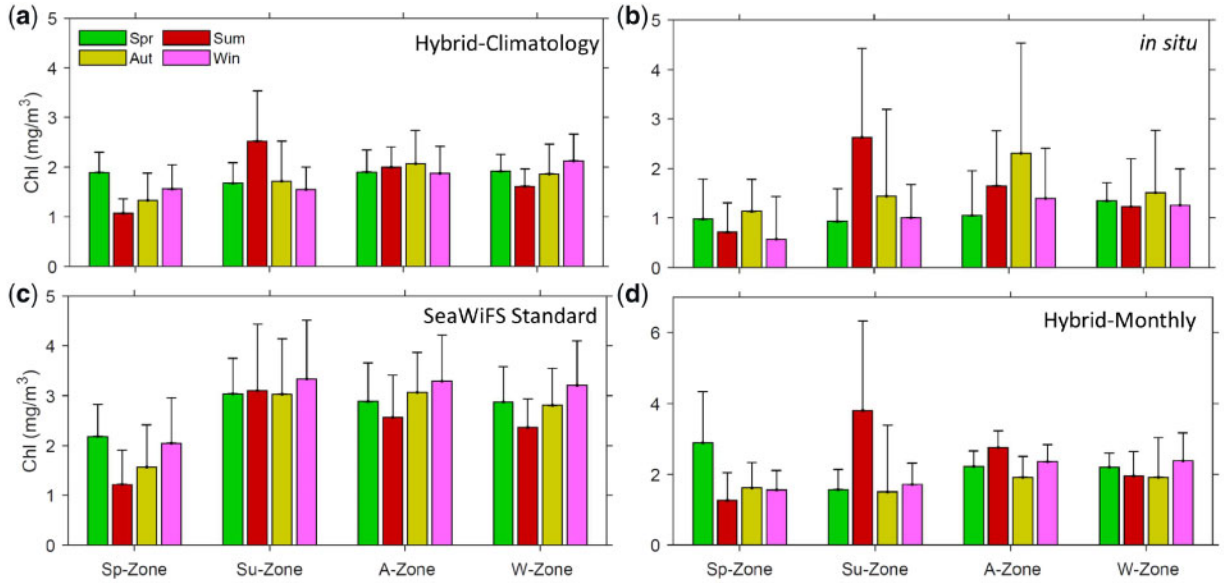

Figure 8. Comparison of seasonal chlorophyll data collected from the Ocean Colour hybrid product, *in situ* and standard SeaWiFS data for subregions with different blooms in the YS. All data are based on the observation points showed in Figure 1. Data used in (a) and (c) are the seasonal mean values derived from climatological products, those in (b) are observations drawn from seasonal cruises running from 2006 to 2007, and those in (d) are monthly mean values of the hybrid product for 2006 to 2007.

in marginal seas. A study similar to this one will allow us to approximate the scale of heterogeneity, to develop better subgrid approximations for large-scale models and to facilitate the development of high-resolution regional models. Second, the need of observations to detect the heterogeneity is substantial. Although our analyses provide a clear picture of spatial patterns of phytoplankton blooms in the YS, the interannual variability of bloom dynamics and their relationships to physical forcings are less clear and warrant further investigation. Although the impact of climate on physical processes in the YS has received much attention (e.g. Wei *et al.*, 2010; Park *et al.*, 2011), more efforts must be made to better understand associated biological responses. Satellite-derived chlorophyll data often present considerable temporal and spatial gaps for the YS, limiting our capacity to detect subtle phenological variabilities in different subregions of the system. This will require the long-term and intensive collection of *in situ* observations from multiple sites in this spatially heterogeneous system, and also the use of multiple phenological indicators to assess the impact by various physical forcings as suggested by Ji *et al.* (2010). Moreover, high-resolution biological–physical modelling focused on bloom dynamics is needed to clearly understand the underlying mechanisms in this dynamically complex and socio-economically important ecosystem (e.g. Ji *et al.*, 2015; Shi *et al.*, 2017).

Limitations and caveats

There are well-known limitations to satellite-derived chlorophyll estimates of coastal waters because of the existence of sediment and coloured dissolved organic matter, which has been a common problem experienced in many similar studies worldwide. The simple empirical ocean colour algorithm has been recommended by Siswanto *et al.* (2011) to improve the accuracy of satellite-derived chlorophyll levels in coastal turbid waters. This approach has been applied in previous studies (Yamaguchi *et al.*, 2013; Zhang *et al.*, 2017) and was also used in this study. Compared with *in situ* chlorophyll data, climatological chlorophyll concentrations estimated from the hybrid algorithm can effectively capture seasonal patterns for most subregions with typical seasonal blooms (Figure 8a and b). Compared with standard SeaWiFS ocean colour data, the new data product also reduces the overestimation of chlorophyll concentrations in areas with high concentrations of suspended sediment (Figure 8a and c). It is worth noting that both survey and satellite data have low spatio-temporal resolutions and may not be sufficient for detecting short-lived blooms. This is evident from the lack of spring blooms represented in data from a single cruise (Figure 8b) and from the lack of autumn blooms missing in monthly SeaWiFS-tuned data (Figure 8d). Future studies will require continuous high-resolution measurements of different biological–physical regimes to better capture the spatial heterogeneity of production processes occurring in marginal seas. This will improve our understanding and projection of future climate impacts on these highly dynamic and important systems.

Summary

The timing of phytoplankton blooms can vary substantially even within a geographically limited marginal sea. Our results show that physical processes such as the YSCWM, CDW, and the YSWC are major drivers of spatial heterogeneity in blooms, mainly through local and remote processes affecting thermal/haline stratifications and nutrient availability in different seasons. Climate-related factors such as seasonal warming/cooling rates may also contribute to the spatial heterogeneity of blooms. Understanding the patterns and drivers of bloom dynamics is critical when discerning the impact of local and remote forcings. Caution should be taken when assessing phytoplankton responses in the context of climate change because of the uncertainty and complexity of underlying mechanisms.

Acknowledgements

Ocean surface chlorophyll and remote sensing reflectance data were obtained from NASA's Ocean Colour website (http://oceancolor.gsfc.nasa.gov/). Sea surface temperature data were derived from NOAA 1/4° daily OISST products (https://www.ncdc.noaa.gov/oisst). This study was supported through NSFC (41306172, 41506185), the Basic Scientific Fund for National Public Research Institutes of China (2014G32), and the Open Fund of CAS KLMEES and QNLM LMEES (KLMEES201604). We thank Mingzhu Fu, Qinsheng Wei, and Zhixuan Feng for their helpful comments and two anonymous reviewers for their valuable feedback.

References

Affan, A., Lee, J-B., Kim, J-T., Choi, Y-C., Kim, J-M., and Myoung, J-G. 2007. Seasonal dynamics of phytoplankton and environmental factors around the Chagwi-do off the West Coast of Jeju Island, Korea. Ocean Science Journal, 42: 117–127.

Beardsley, R. C., Limeburner, R., Yu, H., and Cannon, G. A. 1985. Discharge of the Changjiang (Yangtze River) into the East China Sea. Continental Shelf Research, 4: 57–76.

Behrenfeld, M. J. 2010. Abandoning Sverdrup's critical depth hypothesis on phytoplankton blooms. Ecology, 91: 977–989.

Cebrián, J., and Valiela, I. 1999. Seasonal patterns in phytoplankton biomass in coastal ecosystems. Journal of Plankton Research, 21: 429–444.

Chang, P. H., and Isobe, A. 2003. A numerical study on the Changjiang diluted water in the Yellow and East China seas. Journal of Geophysical Research: Oceans, 108, 3299.

Chen, C-T. A. 2009. Chemical and physical fronts in the Bohai, Yellow and East China seas. Journal of Marine Systems, 78: 394–410.

Chen, S-L., Zhang, G-A., Yang, S-L., and Shi, J. Z. 2006. Temporal variations of fine suspended sediment concentration in the Changjiang River estuary and adjacent coastal waters, China. Journal of Hydrology, 331: 137–145.

Chiswell, S. M. 2011. Annual cycles and spring blooms in phytoplankton: don't abandon Sverdrup completely. Marine Ecology Progress Series, 443: 39–50.

Choi, J. K., and Shim, J. H. 1988. The ecological study of phytoplankton in Kyeonggi Bay, Yellow Sea—IV. The successional mechanism and the structure of the phytoplankton community. Journal of the Korean Society of Oceanography, 23: 1–12.

Clarke, K. R., Somerfield, P. J., and Gorley, R. N. 2016. Clustering in non-parametric multivariate analyses. Journal of Experimental Marine Biology and Ecology, 483: 147–155.

Findlay, H. S., Yool, A., Nodale, M., and Pitchford, J. W. 2006. Modelling of autumn plankton bloom dynamics. Journal of Plankton Research, 28: 209–220.

Fu, M., Sun, P., Wang, Z., Li, Y., and Li, R. 2010. Seasonal variations of phytoplankton community size structures in the Huanghai(Yellow) Sea Cold Water Mass area. Acta Oceanologica Sinica (in Chinese), 32: 120–129.

Fu, M., Wang, Z., Li, Y., Li, R., Sun, P., Wei, X., Lin, X. *et al.* 2009. Phytoplankton biomass size structure and its regulation in the southern Yellow Sea (China): seasonal variability. Continental Shelf Research, 29: 2178–2194.

Gao, S. 2009. Spatial and Seasonal Variation of Chlorophyll and Primary Productivity and Their Controlling Factors in the Northern Yellow Sea (in Chinese). Ocean University of China, Qingdao. 75 pp.

Ho, C., Wang, Y., Lei, Z., and Xu, S. 1959. A preliminary study of the formation of Yellow Sea cold mass and its properties. Oceanologia Et Limnologia Sinica, 2: 11–15.

Holt, J., Hyder, P., Ashworth, M., Harle, J., Hewitt, H. T., Liu, H., New, A. L. *et al.* 2017. Prospects for improving the representation of coastal and shelf seas in global ocean models. Geoscientific Model Development, 10: 499–523.

Hsueh, Y. 1988. Recent current observations in the eastern Yellow Sea. Journal of Geophysical Research: Oceans, 93: 6875–6884.

Huisman, J., van Oostveen, P., and Weissing, F. J. 1999. Critical depth and critical turbulence: two different mechanisms for the development of phytoplankton blooms. Limnology and Oceanography, 44: 1781–1787.

Hyun, J-H., and Kim, K-H. 2003. Bacterial abundance and production during the unique spring phytoplankton bloom in the central Yellow Sea. Marine Ecology Progress Series, 252: 77–88.

Ichikawa, H., and Beardsley, R. C. J. J. o. O. 2002. The current system in the Yellow and East China seas. Journal of Oceanography, 58: 77–92.

Jahan, R., and Choi, J. K. 2014. Climate regime shift and phytoplankton phenology in a macrotidal estuary: long-term surveys in Gyeonggi Bay, Korea. Estuaries and Coasts, 37: 1169–1187.

Jang, P. G., Shin, H. H., Baek, S. H., Jang, M. C., Lee, T. S., and Shin, K. 2013. Nutrient distribution and effects on phytoplankton assemblages in the western Korea/Tsushima Strait. New Zealand Journal of Marine and Freshwater Research, 47: 21–37.

Ji, R., Davis, C. S., Chen, C., Townsend, D., Mountain, D., and Beardsley, R. 2007. Influence of ocean freshening on shelf phytoplankton dynamics. Geophysical Research Letters, 34, L24607.

Ji, R., Edwards, M., Mackas, D. L., Runge, J. A., and Thomas, A. C. 2010. Marine plankton phenology and life history in a changing climate: current research and future directions. Journal of Plankton Research, 32: 1355–1368.

Ji, X., Liu, G., Gao, S., and Wang, H. 2015. Parameter sensitivity study of the biogeochemical model in the China coastal seas. Acta Oceanologica Sinica, 34: 51–60.

Kim, D., Choi, S. H., Kim, K. H., Shim, J., Yoo, S., and Kim, C. H. 2009. Spatial and temporal variations in nutrient and chlorophyll-a concentrations in the northern East China Sea surrounding Cheju Island. Continental Shelf Research, 29: 1426–1436.

Legendre, L. 1990. The significance of microalgal blooms for fisheries and for the export of particulate organic carbon in oceans. Journal of Plankton Research, 12: 681–699.

Lie, H. J. 1984. A note on water masses and general circulation in the Yellow Sea (Hwanghae). The Journal of the Oceanological Society of Korea, 19: 187–194.

Liu, D., and Wang, Y. 2013. Trends of satellite derived chlorophyll-a (1997–2011) in the Bohai and Yellow Seas, China: effects of bathymetry on seasonal and inter-annual patterns. Progress in Oceanography, 116: 154–166.

Liu, X., Chiang, K., Liu, S., Wei, H., Zhao, Y., and Huang, B. 2015a. Influence of the Yellow Sea Warm Current on phytoplankton community in the central Yellow Sea. Deep Sea Research Part I: Oceanographic Research Papers, 106: 17–29.

Liu, X., Huang, B., Huang, Q., Wang, L., Ni, X., Tang, Q., Sun, S. *et al.* 2015b. Seasonal phytoplankton response to physical processes in the southern Yellow Sea. Journal of Sea Research, 95: 45–55.

Lucas, L. V., Koseff, J. R., Monismith, G., Cloern, J. E., and Thompson, J. K. 1999. Processes governing phytoplankton blooms in estuaries. II: the role of horizontal transport. Marine Ecology Progress Series, 187: 17–30.

Miller, C. B. 2004. Biological Oceanography, Blackwell Publishing, Oxford. 402 pp.

Park, S., Chu, P. C., and Lee, J-H. 2011. Interannual-to-interdecadal variability of the Yellow Sea Cold Water Mass in 1967–2008: characteristics and seasonal forcings. Journal of Marine Systems, 87: 177–193.

Pingree, R. D., Holligan, P. M., Mardell, G. T., and Head, R. N. 1976. The influence of physical stability on spring, summer and autumn phytoplankton blooms in the Celtic Sea. Journal of the Marine Biological Association of the United Kingdom, 56: 845–873.

Rabalais, N. N., Turner, R. E., Justić, D., Dortch, Q., Wiseman, W. J., Gupta, B. K. S., and Justic, D. 1996. Nutrient changes in the Mississippi River and system responses on the adjacent continental shelf. Estuaries, 19: 386–407.

Sarmiento, J. L., Slater, R., Barber, R., Bopp, L., Doney, S. C., Hirst, A. C., Kleypas, J. *et al.* 2004. Response of ocean ecosystems to climate warming. Global Biogeochemical Cycles, 18, GB3003.

Shi, J., Liu, Y., Mao, X., Guo, X., Wei, H., and Gao, H. 2017. Interannual variation of spring phytoplankton bloom and response to turbulent energy generated by atmospheric forcing in the central southern Yellow Sea of China: satellite observations and numerical model study. Continental Shelf Research, 143: 257–270.

Siegel, D. A., Doney, S. C., and Yoder, J. A. 2002. The North Atlantic spring phytoplankton bloom and Sverdrup's critical depth hypothesis. Science, 296: 730–733.

Siswanto, E., Tang, J., Yamaguchi, H., Ahn, Y-H., Ishizaka, J., Yoo, S., Kim, S-W. *et al.* 2011. Empirical ocean-color algorithms to retrieve chlorophyll-a, total suspended matter, and colored dissolved organic matter absorption coefficient in the Yellow and East China seas. Journal of Oceanography, 67: 627–650.

Song, H., Ji, R., Stock, C., and Wang, Z. 2010. Phenology of phytoplankton blooms in the Nova Scotian Shelf–Gulf of Maine region: remote sensing and modeling analysis. Journal of Plankton Research, 32: 1485–1499.

Song, H., Ji, R., and Wang, Z. 2011. A review of coastal phytoplankton bloom dynamics and phenology. Advances in Earth Science (in Chinese), 26: 257–265.

Song, H., Zhang, X., Wang, B., Sun, X., Wang, X., and Xin, M. 2014. Bottom-up and top-down controls of the phytoplankton standing stock off the Changjiang Estuary. Acta Oceanologica Sinica (in Chinese), 36: 91–100.

Stock, C. A., Alexander, M. A., Bond, N. A., Brander, K. M., Cheung, W. W. L., Curchitser, E. N., Delworth, T. L. *et al.* 2011. On the use of IPCC-class models to assess the impact of climate on living marine resources. Progress in Oceanography, 88: 1–27.

Su, J., and Yuan, Y. 2005. Hydrography of China Seas (in Chinese). China Ocean Press, Beijing.

Sverdrup, H. U. 1953. On conditions for the vernal blooming of phytoplankton. Journal du Conseil International pour l'Exploration de la Mer, 18: 287–295.

Tassan, S. 1994. Local algorithms using SeaWiFS data for the retrieval of phytoplankton, pigments, suspended sediment, and yellow substance in coastal waters. Applied Optics, 33: 2369–2378.

Wang, B., Wang, X., and Zhan, R. 2003. Nutrient conditions in the Yellow Sea and the East China Sea. Estuarine, Coastal and Shelf Science, 58: 127–136.

Wei, H., Shi, J., Lu, Y., and Peng, Y. 2010. Interannual and long-term hydrographic changes in the Yellow Sea during 1977–1998. Deep Sea Research Part II: Topical Studies in Oceanography, 57: 1025–1034.

Wei, Q., Yu, Z., Wang, B., Fu, M., Xia, C., Liu, L., Ge, R. *et al.* 2016. Coupling of the spatial–temporal distributions of nutrients and physical conditions in the southern Yellow Sea. Journal of Marine Systems, 156: 30–45.

Winder, M., and Cloern, J. E. 2010. The annual cycles of phytoplankton biomass. Philosophical Transactions of the Royal Society B: Biological Sciences, 365: 3215–3226.

Winder, M., and Sommer, U. 2012. Phytoplankton response to a changing climate. Hydrobiologia, 698: 5–16.

Wood, S. N. 2006. Generalized Additive Models: An Introduction with R. Chapman and Hall/CRC Press, Baca Raton.

Xin, M., Ma, D., and Wang, B. 2015. Chemicohydrographic characteristics of the Yellow Sea Cold Water Mass. Acta Oceanologica Sinica, 34: 5–11.

Xu, Q., Sukigara, C., Goes, J. I., do Rosario Gomes, H., Zhu, Y., Wang, S., Shen, A. *et al.* 2019. Interannual changes in summer phytoplankton community composition in relation to water mass variability in the East China Sea. Journal of Oceanography, 75: 61–79.

Yamaguchi, H., Ishizaka, J., Siswanto, E., Son, Y. B., Yoo, S., and Kiyomoto, Y. 2013. Seasonal and spring interannual variations in satellite-observed chlorophyll-a in the Yellow and East China seas: new datasets with reduced interference from high concentration of resuspended sediment. Continental Shelf Research, 59: 1–9.

Yamaguchi, H., Kim, H-C., Son, Y. B., Kim, S. W., Okamura, K., Kiyomoto, Y., and Ishizaka, J. 2012. Seasonal and summer interannual variations of SeaWiFS chlorophyll a in the Yellow Sea and East China Sea. Progress in Oceanography, 105: 22–29.

Yang, E. J., Choi, J. K., and Hyun, J-H. 2008. Seasonal variation in the community and size structure of nano- and microzooplankton in Gyeonggi Bay, Yellow Sea. Estuarine, Coastal and Shelf Science, 77: 320–330.

Yang, X., Xue, Y., Zan, X., and Ren, Y. 2014. Community structure of phytoplankton in Haizhou Bay and adjacent waters and its relationships with environmental factors. Chinese Journal of Applied Ecology (in Chinese), 25: 2123–2131.

Yuan, D., Zhu, J., Li, C., and Hu, D. 2008. Cross-shelf circulation in the Yellow and East China Seas indicated by MODIS satellite observations. Journal of Marine Systems, 70: 134–149.

Zhang, H., Qiu, Z., Sun, D., Wang, S., and He, Y. 2017. Seasonal and interannual variability of satellite-derived chlorophyll-a (2000–2012) in the Bohai Sea, China. Remote Sensing, 9: 582.

Zhang, J., Liu, S. M., Ren, J. L., Wu, Y., and Zhang, G. L. 2007. Nutrient gradients from the eutrophic Changjiang (Yangtze River) estuary to the oligotrophic Kuroshio waters and re-evaluation of budgets for the East China Sea shelf. Progress in Oceanography, 74: 449–478.

Zhou, M., Shen, Z., and Yu, R. 2008. Responses of a coastal phytoplankton community to increased nutrient input from the Changjiang (Yangtze) River. Continental Shelf Research, 28: 1483–1489.

Handling editor: Shubha Sathyendranath